

The impact of a high birefringence section in an optical network system through emulation

Vitalis Musara, Lorinda Wu, Gaoboelwe Pelaelo and Andrew W. R. Leitch

Department of Physics, Nelson Mandela Metropolitan University, P. O. Box 77000, Port Elizabeth, 6031, South Africa, Tel: +27 41 5042141; Fax: +27 41 5042573; email: Vitalis.Musara@nmmu.ac.za

Abstract — Polarization mode dispersion (PMD) contributions by each birefringent fibre section on an optical network link can be best analyzed through PMD emulation. A sub-emulator was design from coupling sections of polarization maintaining fibres (PMFs) to mimic the DGD behaviour in a deployed fibre. To show the impact of a high birefringent (HiBi) fibre in an optical network a 23 m single PMF section is coupled to the sub-emulator via a polarization controller (PC). Results show that the RMS-DGD of the emulator is always ~ 31 ps which is close to that given by the HiBi section. Simultaneous adjustments in the maximum and minimum values of the DGD statistics are also achieved. We go further to show that the presence of a HiBi section in an optical link can shift the DGD statistics away from the Maxwellian distribution.

Index Terms — birefringence, emulator, mode coupling, polarization mode dispersion.

I. INTRODUCTION

Polarization mode dispersion (PMD) is of major concern due to current and future increases in bit-rate transmission, 10 Gb/s and above. PMD is defined as the differential group delay (DGD) between the fast and slow principal states of polarization (PSP) along an invariant unit Stokes vector [1]. DGD is the magnitude of the PMD vector. In order to understand the PMD behaviour and its impact on network performance, it is vital to perform PMD emulation under a controlled environment.

Gisin *et al.* [2] first showed that the DGD statistics in optical network systems follow a Maxwellian distribution. This is possible if there is infinite random mode coupling. In order to mimic the DGD statistics exhibited by deployed fibres researchers have designed PMD emulators through cascading polarization maintaining fibre (PMF) segments [3,4,5]. These emulators generate DGD statistics that approach the theoretical Maxwellian distribution. The condition of these emulator designs is that the length of each PMF segment should lie within a 20% standard deviation of the mean length. Mode coupling is random and the PMF lengths are Gaussian distributed. This might not be the case in deployed fibres, with some segments having higher birefringence (HiBi) compared to the others [6,7].

Huttner *et al.* [6] and Conibear *et al.* [7] observed the existence of HiBi fibre sections in optical networks through the use of a polarization optical time domain reflectometry (P-OTDR). These HiBi sections have greater polarization impact on propagating signals than the low birefringence sections that make up the rest of the fibre link. Therefore there must be careful analysis and evaluation of PMD contributions in fibre links. Replacement or re-routing of only these HiBi sections instead of removing the entire fibre link is a cost effective approach to network upgrade.

To our understanding researchers have not well understood the impacts generated by these HiBi segments, on the mean DGD value and the nature of the DGD statistics. In order to address this, we present a low-cost emulator from combining a sub-emulator, a polarization controller (PC) and a very HiBi fibre segment. We do not pay only particular attention on monopolizing the root mean square (RMS)-DGD values but our design extends in altering the extreme DGD values (max and min) of the DGD statistics.

II. THEORY BEHIND EMULATOR OPERATION

The emulator constitutes a variable sub-emulator (made up from cascading polarization maintaining fibre (PMF) segments), a variable PC and a 23 m long PMF HiBi fibre section (fixed length) as shown in Fig. 1. The PMF has a PMD coefficient of ~ 1.35 ps/m.

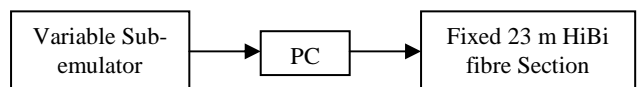


Fig. 1: Block diagram for an emulator with fixed RMS-DGD with varying DGD spectra. The PC angle is set fixed at $\pi/4$.

The variable sub-emulator is tuned by joining or removing PMF fibre segments. The length of each PMF segment lies within 20% of the mean length of the sub-emulator in a similar manner to other emulator designs [3,4,5]. The PC provides a coupling angle ϕ between the sub-emulator and the HiBi fibre sections. The RMS-DGD of the variable sub-emulator varies from 4 - 13.2 ps and that of the fixed HiBi fibre section is ~ 31 ps. The RMS-DGD = $(\langle \text{DGD}^2 \rangle)^{1/2}$, where $\langle \rangle$ denotes the average. The length of the HiBi fibre section was by far out of the 20% standard deviation of the mean length of the emulator, which is contrary to conditions we used to construct the sub-emulator.

The global (or overall) PMD vector $\vec{\tau}_{global}(\omega)$ of the entire emulator can be expressed as [8]:

$$\vec{\tau}_{global}(\omega) = \vec{m}_{out}^N \quad (1)$$

where

$$\begin{aligned} \vec{m}_{out}^N = & \Delta\tau_N \vec{e}_N + \left(\vec{m}_{out}^{N-1} \cdot \vec{e}_N \right) \vec{e}_N + \cos(2\Delta\tau_N \omega) \times \\ & \left[\vec{m}_{out}^{N-1} - \left(\vec{m}_{out}^{N-1} \cdot \vec{e}_N \right) \vec{e}_N \right] - \sin(2\Delta\tau_N \omega) \vec{e}_N \times \vec{m}_{out}^{N-1} \end{aligned} \quad (2)$$

where N is the number of PMF segments ($N = 1, 2, 3 \dots$). m_{out} is the outgoing state of polarization (SOP). $\Delta\tau_N$ is the DGD of the N -th fibre segment. \vec{m}_{out} is related to \vec{m}_{in} (incoming SOP) by a rotational angle $2\Delta\tau_N \omega$ around a unit vector \vec{e}_N , while ω is the optical angular frequency. Eqn. (1) also applies to the sub-emulator.

For $N = 1$ we consider the emulator to maintain its PSPs unchanged and for $N = 2$ the PSPs are wavelength (λ) dependent whilst the DGD is independent of λ (see Fig. 3). This is in agreement with Gisin *et al.* [8], Zeng [9] and Wegmuller *et al.* [10] who assumed the two PMD vectors from the two fibre sections ($N = 2$) to be independent of λ . For $N > 2$ both the principal states of polarization (PSPs) and DGD become λ -dependent (refer to Fig. 3). The λ -dependency by the PMD vectors is due to our variable sub-emulator comprising of several λ dependent components (when $N > 2$). The single 23 m HiBi fibre section alone has a PMD vector independent of λ . This emulator is closer to reality compared to Zeng [9] and Wegmuller *et al.*'s [10] designs since DGD statistics in deployed fibres are λ -dependent. This is due to the presence of numerous random birefringent segments and mode coupling variations.

The PC angle ϕ was maintained at $\pi/4$ throughout the entire experiment. This angle resulted in the emulator giving a RMS-DGD value fairly close to its RMS-value as the numbers of sections on the variable sub-emulator were varied from 1 to 30. Other angles can still give RMS-DGD values fairly close to that of the HiBi section. The PMF length distribution in the variable sub-emulator is random. Mode coupling is assumed to be random since the exact coupling angles could not be determined when fusion splicing the PMF segments. Due to these unknown coupling angles it is difficult to calculate or predict the amount of DGD using Eq. (1).

We used the frequency domain Jones Matrix Eigenanalysis [11] PMD measurement technique under stable conditions over a 1520-1570 nm λ range (at a λ resolution of 0.3 nm) to analyse our emulator.

III. RESULTS AND DISCUSSION

A. The sub-emulator

Fig. 2 shows the measured properties of the variable sub-emulator alone. As the number of coupled PMF sections are increased from 1 – 30 there is increased birefringence. This results in increased DGD just as an optical delay line

increases its birefringence. This is well supported by Fig. 2 (a) where the RMS-DGD increases from 4 to 13.2 ps. There are also more stochastic DGD changes generated due to increased random mode coupling, which results in the DGD statistical behaviour approaching the Maxwellian distribution. Thus a better approach to the Maxwell distribution is achieved when there are 30 PMF segments, refer to Fig. 2 (b). The presence of uniform mode coupling and PMF lengths on the sub-emulator would give periodic DGD changes which are not a good representation of deployed fibres.

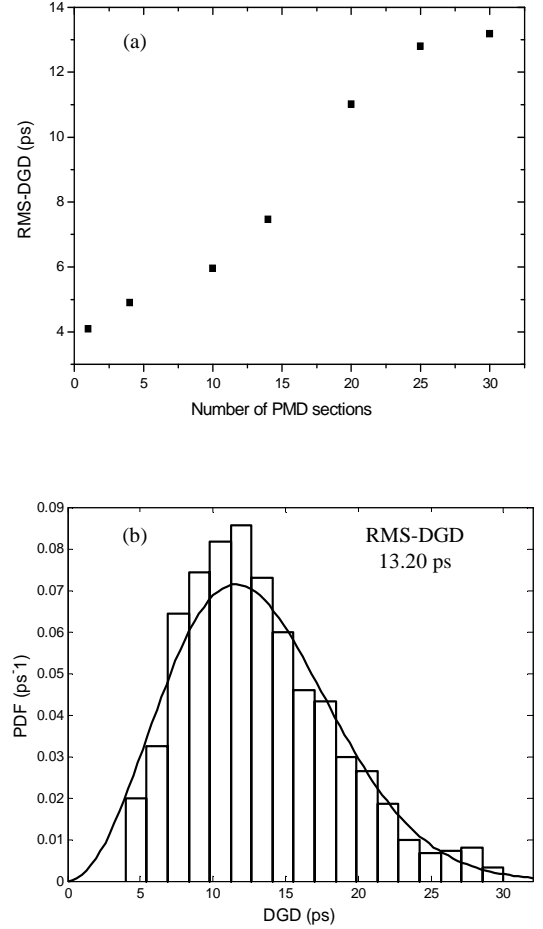


Fig. 2: (a) The DGD variation as the number of PMF segments on the sub-emulator increase from 1 - 30. (b) The DGD histogram for the sub-emulator alone, with 30 segments. The solid line represents the Maxwell distribution.

We therefore deduce that continued increase in random mode coupling will give DGD statistics approximating Maxwellian. The RMS-DGD magnitude is independent of whether DGD statistics approach the Maxwell distribution or not. The key factor is sufficient random mode coupling.

B. The emulator

An adjustment (from 1 - 30 segments) on the variable sub-emulator whilst it is attached to the fixed HiBi fibre via the PC increases PMD stochastic changes, see Fig. 3. These irregular DGD fluctuations occur around a fixed RMS-DGD. These fluctuations are likely attributed to the presence of higher-order PMD. This has already been discovered by other researchers [12,13]. Any changes in the sub-emulator

mode coupling angles (which should always remain non-correlated) would highly affect the DGD spectrum but slightly if not the RMS-DGD value. This is due to the dominant PMD vector emanating from the HiBi segment.

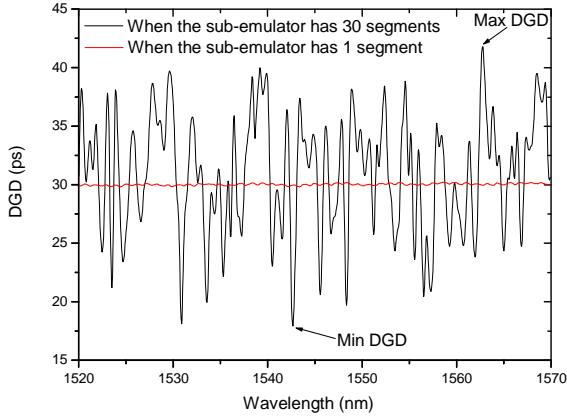


Fig. 3: The DGD λ spectrum for the emulator when there are 1 and 30 PMF segments on the sub-emulator. The arrows show how the max and min values are determined from a DGD spectrum. The RMS-DGD is calculated.

Contrary to our expectations the DGD distribution in Fig. 4 (a) approaches a Weibull distribution instead of the Maxwellian distribution when the sub-emulator has 30 segments. The Weibull distribution looks like a reversed Maxwellian distribution, with a low probability events tail for low DGD. We suspect the DGD statistics deviates from the statistics in Fig. 2 (b) due to high contributions from the dominant PMD vector of the HiBi fibre section. This is true as Fig. 4 (b) shows an illustration of a constant RMS-DGD equal to 31.2 ± 0.9 ps with either an increase or decrease in the number of birefringent segments on the sub-emulator. The other number of PMF segments (less than 30) on the sub-emulator resulted in the emulator giving other different distributions which possess high DGD values. This means there are more possibilities of high system impairments due to high DGD values more likely to occur, e.g. see the right hand tail of Fig. 4 (a). This also shows that in deployed fibres different mode coupling and birefringence contributions in the presence of such a HiBi section would lead to different DGD distributions centred fairly at the same RMS-DGD value. These distributions would cover different DGD ranges.

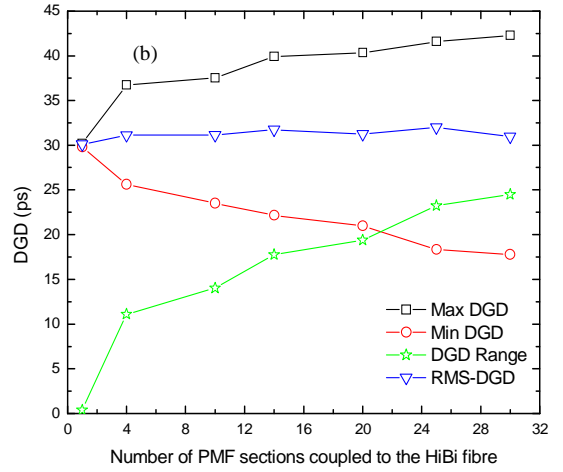
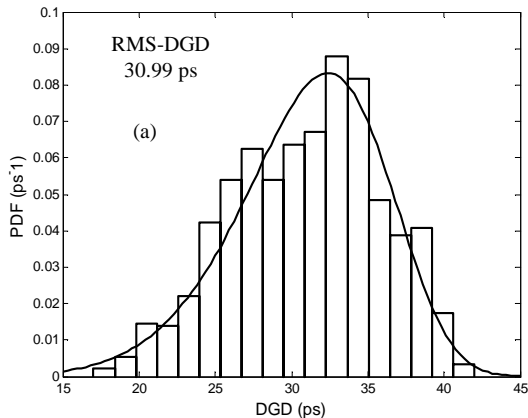


Fig. 4: (a) The DGD histogram when the emulator has 30 segments on its sub-emulator. The solid line represents the Weibull distribution. (b) The DGD statistical values for the emulator as the number of PMF segments (1 - 30) are concatenated to the 23 m HiBi fibre section.

The min DGD value in Fig. 4 (a) is greater than that in Fig. 2 (b), indicating a shift in the DGD statistics occurs towards the dominant λ -independent PMD vector. We suspect during this shift there were DGD statistical changes from Fig. 2 (b) to Fig. 4 (a). Therefore this means a section with a dominant PMD vector in an optical network biases DGD measurements towards its RMS-DGD value. This does not give a true representation of contributions from all concatenated fibre segments making up an entire optical fibre link.

We therefore propose that in order to get a Maxwellian distribution from such a design we need to extend the min DGD to zero and generate further DGD stochastic changes. This would be achieved by increasing the number of PMF segments on the sub-emulator. These PMF sections should be of random length and mode coupling. Thus in such a case the HiBi section might not have profound effect on the DGD statistical behaviour but only on the RMS-DGD value. Therefore this means deployed fibres comprising a HiBi section can still approach a Maxwellian distribution when there is numerous mode coupling. This would mean DGD contributions from fibre segments along the fibre link length should always be analysed carefully no matter if the DGD statistics approach the predictable Maxwellian distribution.

To give an insight in the DGD behaviour in an optical fibre link with a HiBi section assuming both mode coupling and birefringence increase, refer to Fig. 4 (b). This was achieved through emulation. Fig. 4 (b) shows that the RMS-DGD is equal to the max and min DGD values when there is no mode coupling. The DGD range increases as can be seen by the increasing separation between the min and max DGD from the constant RMS-DGD value. This is due to an increase in the number of PMF segments on the sub-emulator. We therefore conclude that a continued increase in the number of coupled PMF segments on the sub-emulator will result in the min DGD approaching 0 and the max DGD approaching higher values. Thus under these conditions we

expect the DGD range to be equal to the max DGD value. The RMS-DGD remains fairly constant at 31.2 ± 0.9 ps.

Future work involves improving the emulator to generate a DGD Maxwellian distribution. This will also involve an investigation into the exact amount of birefringence just sufficient enough to start drifting the DGD behaviour away from the Maxwellian distribution.

IV. CONCLUSIONS

The sub-emulator shows that increased random mode coupling and PMF segments give a DGD statistics approaching the Maxwell distribution. This is true when the lengths of the PMF segments lie within the 20% standard deviation of the mean length. The emulator shows that the the 23 m HiBi fibre section shifted the sub-emulator DGD statistics towards its RMS-DGD value. This resulted in the emulator DGD statistics approaching unpredictable statistical distributions instead of the anticipated predictable Maxwellian distribution even when there was presence of random mode coupling. These distributions show that high DGD values have more chances of occurrence which means there are higher possibilities of system impairments. However, the emulator is novel since we can simultaneously tune the DGD statistics horizontally (DGD changes with wavelength) and vertically (the DGD range) whilst maintaining the RMS-DGD fairly fixed.

ACKNOWLEDGMENT

This project forms part of the Telkom Centre of Excellence at Nelson Mandela Metropolitan University (NMMU) and is financially supported by Telkom South Africa Ltd, Ingoma Communications Services (Pty) Ltd, Hezeki Contracting (Pty) Ltd, MCT Telecommunications (Pty) Ltd and THRIP.

REFERENCES

- [1] C. D. Poole and R. E. Wagner, 'Phenomenological approach to polarization dispersion in long single-mode fibers,' *Electron. Lett.* **22** (1986) 1029.
- [2] N. Gisin, R. Passy, J.C. Bishoff, and B. Perny, 'Experimental investigations of the statistical properties of polarization mode dispersion in single mode fibers,' *IEEE Photon. Technol. Lett.* **5** (1993) 819
- [3] R. Khosravani, I. T. Lima, P. Ebrahimi, E. Ibragimov, A. E. Willner and C. R. Menyuk, 'Time and Frequency Domain characteristics of Polarization-Mode Dispersion Emulators,' *IEEE Photon. Technol. Lett.* **13** (2001) 127
- [4] L.-S. Yan, B. Zhang, X. Steve Yao and A. E. Willner, 'Reducing the number of polarization controllers in all-fiber polarization-mode-dispersion emulators using polarization maintaining fiber subsections with unequal lengths,' *Opt. Fiber Technol.* (2007) doi:10.1016/j.yofte.2007.11.004
- [5] B. S. Marks, I. T. Lima, and Jr C. R. Menyuk, 'Autocorrelation Function for PMD Emulators with rotators,' *CLEO2002 CWH5* (2002) 397

- [6] B. Huttner B., Gisin B. and Gisin N., 'Distributed PMD measurements with a polarization-OTDR in optical fibers,' *J. Lightwave Technol.* **17** (1999) 1843
- [7] A.B. Conibear, A. W. R. Leitch, N. A. Sibaya, T. B. Gibbon and L. Viljoen, 'Study of polarization mode dispersion in a South African optical fibre network,' *S.A. J. of Science* **101** (2005) 275
- [8] N. Gisin and J. P. Pellaux, 'Polarization mode dispersion: time versus frequency domains,' *Opt. Comm.* **89** (1992) 316
- [9] K. C. Zeng, 'A PMD Emulator With Tunable Second-Order PMD and Constant Mean First-Order DGD,' *IEEE Photon. Technol. Lett.* **15** (2003) 1150
- [10] M. Wegmuller, S. Demma, C. Vinegoni, and N. Gisin, 'Emulator of First-and Second-Order Polarization-Mode Dispersion,' *IEEE Photon. Technol. Lett.* **14** (2002) 630
- [11] B. L. Huffner, 'Automated measurement of polarization mode dispersion using Jones matrix eigenanalysis,' *IEEE Phpn. Technol. Lett.* **4** (1992) 1066
- [12] F. Buyère, 'Impact of first and second order PMD in optical digital transmission systems,' *Opt. Fiber Technol.* **2** (1996) 269
- [13] L. E. Nelson, R. M. Jopson and H. Kogelnik, 'Polarization mode dispersion penalties associated with rotation of principal states of polarization in optical fiber,' *Proc OFC 2000 ThB2* (2000) 25

Vitalis Musara graduated with a BSc Honours in Physics in 2004 and an MSc in Applied Physics in 2006. He is a PhD student at Nelson Mandela Metropolitan University. His interests are polarization studies of optical fibres, networking and electronics.